INL/CON-11-24025
PREPRINT

Improved Computational Neutronics Methods and Validation Protocols for the Advanced Test Reactor

PHYSOR 2012

David W. Nigg
Joseph W. Nielsen
Benjamin M. Chase
Ronnie K. Murray
Kevin A. Steuhm
Troy Unruh

April 2012

The INL is a
U.S. Department of Energy
National Laboratory
operated by
Battelle Energy Alliance

PHYSOR 2012 – Advances in Reactor Physics – Linking Research, Industry, and Education
Knoxville, Tennessee, USA, April 15-20, 2012, on CD-ROM, American Nuclear Society, LaGrange Park, IL (2012)

IMPROVED COMPUTATIONAL NEUTRONICS METHODS AND VALIDATION PROTOCOLS FOR THE ADVANCED TEST REACTOR

David W. Nigg, Joseph W. Nielsen, Benjamin M. Chase, Ronnie K. Murray, Kevin A. Steuhm, Troy Unruh
Idaho National Laboratory
2525 Fremont Street
Idaho Falls, ID 83415-3870
dwn@inel.gov

ABSTRACT

The Idaho National Laboratory (INL) is in the process of updating the various reactor physics modeling and simulation tools used to support operation and safety assurance of the Advanced Test Reactor (ATR). Key accomplishments so far have encompassed both computational as well as experimental work. A new suite of stochastic and deterministic transport theory based reactor physics codes and their supporting nuclear data libraries (HELIOS, KENO6/SCALE, NEWT/SCALE, ATTILA, and an extended implementation of MCNP5) has been installed at the INL. Corresponding models of the ATR and ATRC are now operational with all five codes, demonstrating the basic feasibility of the new code packages for their intended purposes. On the experimental side of the project, new hardware was fabricated, measurement protocols were finalized, and the first four of six planned physics code validation experiments based on neutron activation spectrometry have been conducted at the ATRC facility. Data analysis for the first three experiments, focused on characterization of the neutron spectrum in one of the ATR flux traps, has been completed. The six experiments will ultimately form the basis for flexible and repeatable ATR physics code validation protocols that are consistent with applicable national standards.

Key Words: ATR, Validation, Experiments

1.0 INTRODUCTION

The Advanced Test Reactor (ATR), located at the Idaho National Laboratory (INL), has a variety of missions involving accelerated testing of nuclear fuel and other materials in a high neutron flux environment, medical and industrial isotope production, etc. Along with its companion critical mockup (ATRC), the ATR is one of the key research and testing facilities within the US Department of Energy (DOE) National Laboratory Complex. The ATR and ATRC also serve as the centerpieces of the recently-formed ATR National Scientific User Facility (NSUF), whose purpose is to facilitate the current trend toward broadening the applications of the ATR beyond its traditional base.

The ATR (Figure 1) is a heterogeneous light-water and beryllium moderated, beryllium reflected, light-water cooled system with 40 highly-enriched (93% ^{235}U) plate-type fuel elements arranged in a serpentine pattern. Gross reactivity and power distribution control during operation is achieved through the use of eight pairs of rotating control drums with hafnium neutron absorber plates on one side as can be seen in Figure 1. There are several flux traps to provide high thermal neutron fluxes for irradiation of experiments. The rated operating power is 250 MW. Typical thermal neutron fluxes in the flux traps can be as high as 5.0×10^{14} n/cm^2-s.

Typical operating cycle lengths are in the range of 45–60 days. The core fuel configuration and the experiment loadings are usually rearranged between cycles, and each fuel element is typically burned for two or three cycles during its useful lifetime.

The ATRC (Figure 2) is an open-pool mock-up of the ATR that typically operates at approximately 600 W and produces thermal neutron flux levels in the traps that are in the range of 1.0×10^9 n/cm^2-s. The ATRC facility is typically used with prototype experiments to characterize in advance, with precision and accuracy, the expected changes in core reactivity for the same experiments in the ATR itself. Useful physics data can also be obtained for evaluating the worth and calibration of control elements as well as thermal and fast neutron distributions in the core.

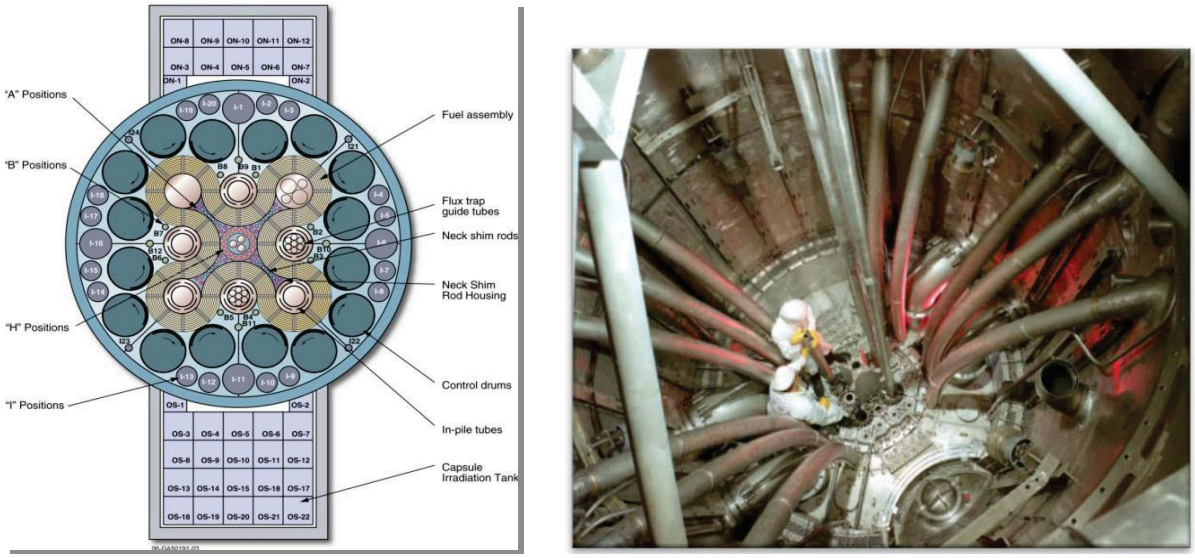

Figure 1. Core and reflector geometry of the Advanced Test Reactor showing the various flux traps (L), and view into the reactor vessel during construction (R).

Computational reactor physics modeling is used extensively to support ATR experiment design, operations and fuel cycle management, core and experiment safety analysis, and many other applications. Experiment design and analysis for the ATR is generally supported by very detailed and sophisticated three-dimensional Monte Carlo analysis, typically using the internationally recognized continuous-energy MCNP5 code [1] coupled to extensive fuel isotope buildup and depletion analysis where appropriate. In contrast, the computational reactor physics software tools and protocols currently used for ATR core fuel cycle analysis and operational support are largely based on four-group diffusion theory in two-dimensional Cartesian geometry [2], with heavy reliance on "tuned" nuclear parameter input data and various empirical correlations for converting the computational output into useful operating parameters and limits.

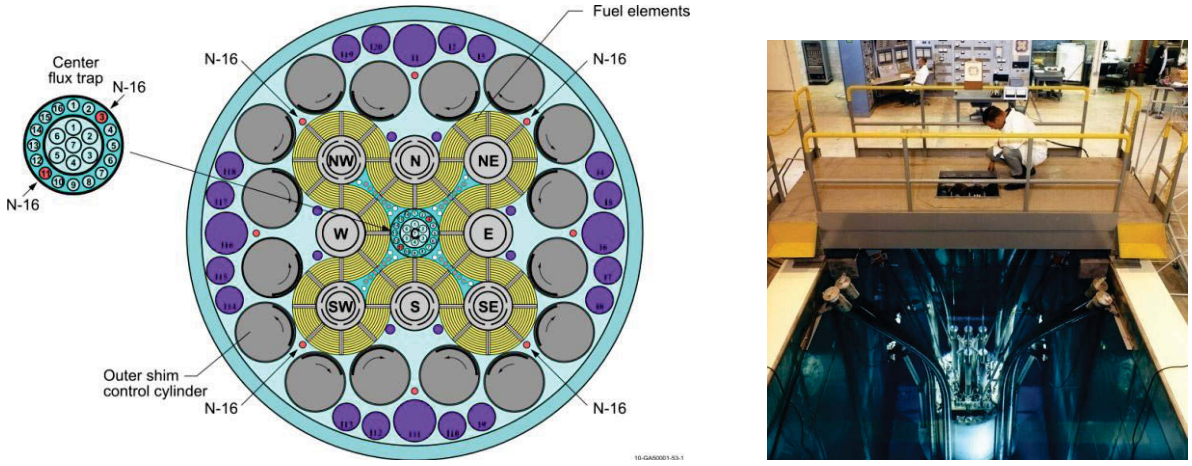

Figure 2. Core and reflector geometry of the Advanced Test Reactor Critical Facility (L), and view into the ATRC reactor pool (R).

Thus the historical approach to ATR reactor physics operational support is inconsistent with the state of modern nuclear engineering practice and problematic to verify and validate (V&V) according to current international standards. Furthermore, some aspects of the analysis process are highly empirical in nature as noted above, with many "correction factors" and approximations that require very specialized experience to apply. Finally, future clients of the ATR NSUF are anticipated to be experienced in the use of modern computational methods available for nuclear systems modeling and are likely to expect corresponding computational support services within the NSUF infrastructure. Accordingly efforts are currently underway to improve the overall approach to computational neutronics modeling of the ATR core, with the following specific objectives:

- Implementation of complementary, self-consistent multidimensional stochastic and deterministic neutron transport models of the ATR and ATRC cores using well-established and recognized science-based software packages consistent with current engineering practice
- Standardized computational protocols and training, more easily transferred to new staff members
- Additional V&V, with development of apparatus and protocols for detailed neutron flux distribution and spectrum validation measurements in the core and selected flux traps that can be adapted as needed for changing experimental conditions and repeated on a regular basis.

Figure 3 shows the suite of new tools that will be available and how they generally relate to one another. The most recent release of the Evaluated Nuclear Data Files (ENDF/B Version 7) will be used to provide the basic cross section data and other nuclear parameters required for all of the modeling codes. The ENDF files are processed into computationally-useful formats using the NJOY or AMPX codes [3] as applicable.

As noted earlier, the MCNP5 three-dimensional stochastic simulation code is already used extensively for ATR experiment design and analysis and, to some limited extent, core analysis. The KENO6 stochastic simulation code [4] is also being introduced, primarily for detailed core analysis in connection with ongoing ATR and ATRC operations as well as for support of the possible conversion of the ATR to low-enrichment uranium (LEU) fuel. KENO6 is useful both as a stand-alone analysis and verification tool as well as in conjunction with the TSUNAMI [5] sensitivity-uncertainty analysis system available with the SCALE [6] nuclear system analysis package.

The right-hand side of Figure 3 shows the new high-fidelity multidimensional deterministic transport computational tools that are being integrated into the system. HELIOS [7] and ATTILA [8] are commercial grade software products now in place at the INL under permanent sitewide licenses. NEWT [9], together with its SCALE-based support infrastructure and the TRIDENT [6] depletion methodology, is a well-established and verified software tool developed within the DOE National Laboratory system. Taken together, these three code packages will provide the necessary high-fidelity neutron and gamma transport capability that is required for various aspects of ATR and ATRC core physics and ATR fuel cycle modeling.

The modeling upgrade efforts underway also include several activities designed to incorporate historical validation data from earlier ATR and ATRC experiments as well as to develop new validation data specific to the new computational models and protocols. In particular, much of the initial model development has been based on a very well documented ATR critical experiment conducted as part of the 1994 ATR Core Internals Changeout (CIC) activity [10]. New measurements in the ATRC are also underway, and the combined results of the first three new validation experiments, focused on detailed characterization of the neutron flux in the Northwest Large In-Pile Tube (NW-LIPT) are summarized in this paper.

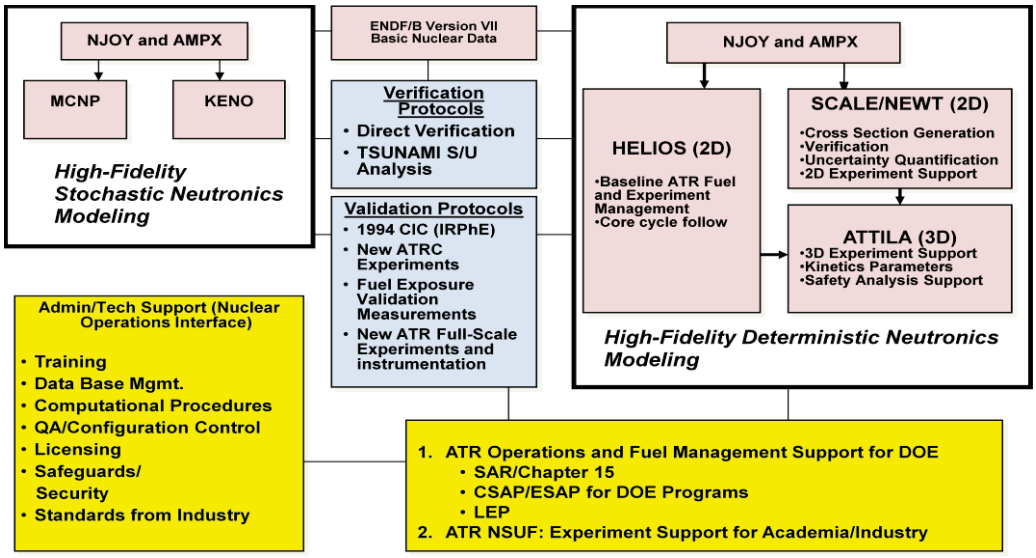

Figure 3. Advanced computational tool suite for the ATR and ATRC, with supporting verification, validation and administrative infrastructure.

2.0 METHODS AND MATERIALS

Validation protocols for the various computational models are based on neutron activation spectrometry. Some new equipment for detailed activation experiments in the NW LIPT has been fabricated and initial scoping measurements have been completed. Ultimately a standard set of experimental apparatus and associated validation measurement protocols will be available for future code and model validation as needed in both the ATRC and, when feasible, in the ATR itself. The work described here builds on extensive previous relevant INL experience at the ATR [11] as well as at other research reactor and accelerator facilities worldwide [12]

2.1 Experimental Apparatus

In the initial phase of the experimental campaign described here various sets of activation foils and wires were irradiated in the NW LIPT of the ATRC, with a "balanced" outer shim critical configuration (all drums at the same angular rotation relative to the fuel). Three 20-minute ATRC reactor runs at 600 watts were required for this phase. Activation responses included in the measurements are listed in Table 1. The first irradiation was targeted on the thermal and epithermal neutron energy range and included duplicate bare Au and Mn foils and duplicate cadmium-covered In, Au, W, Mn, and Cu foil packages. The second irradiation was conducted primarily to experimentally confirm the anticipated small effect of the cadmium-covered foil packages used in Irradiation 1 on the local flux in the NW LIPT. The third irradiation was designed to provide additional spectral detail in the energy range above about 300 keV using a set of In, Ti, Ni, Zn, Fe, and Nb foils contained within a hollow spherical spectral shifting shield composed of boron. The foils were standard 12.7 mm (0.5") diameter foils with thicknesses ranging from 0.0254 mm (1 mil) to 0.127 mm (5 mil).

The foils were positioned within the ATRC NW LIPT insert using specialized insert fittings fabricated for this purpose. Foils used for thermal and epithermal neutron measurements during Irradiation 1 were placed in two covered aluminum strips (Figure 4). These strips fit into the middle slots of the square holder shown on the right-hand side of Figure 5, which fits, in turn, into the square cavity in the cylindrical LIPT insert on the left hand side of Figure 5. The Cd-covered packages were placed in the upper position in the first strip and in the lower position in the second strip. This placement pattern was reversed for the bare foil packages, enabling quantification and averaging of any flux differences that that may exist between the upper and lower positions due to axial gradients. The insert fitting also contains "dummy" strips in the other eight positions as shown in Figure 5. These dummy strips are designed so that the fully-assembled insert fitting will have the same metal-to-water ratio as it has in the case of the third irradiation, where a second positioning device, for the boron spectral shield, is substituted in the place of the foil holding strips and dummies used in the first and second irradiations.

Copper/gold (1.55% Au by weight alloyed in natural Cu) flux wires were also placed at specific locations within the strips as shown in Figure 4. These wires were 1 mm in diameter and approximately 0.635 cm (0.25") in length. They each contain approximately 45 milligrams of natural copper and 0.7 milligrams of gold. The wires were used to obtain a common measure of the fast and thermal neutron flux in the experiment hardware from one irradiation to another.

Table 1. Activation interactions of interest for ATR model validation applications

Neutron Interaction	Nominal Mass and Composition of Standard Foil	Half-life of Product of Interest	Energy Range of Primary Response	Activation Gamma Energy of Interest (keV)
^{115}In (n, γ)^{116}In	25 mg, 100% In	54 Minutes	1 eV Resonance	1293,1097, 416
^{197}Au (n, γ)^{198}Au	60 mg, 100% Au	2.694 Days	Thermal & 5 eV Resonance	412
^{186}W(n, γ)^{187}W	60 mg, 100% W	23.9 Hours	18 eV Resonance	686
^{55}Mn(n, γ)^{56}Mn	50 mg, 80% Mn, 20% Cu	2.578 Hours	Thermal & 340 eV Resonance	847
^{63}Cu (n, γ)^{64}Cu	140 mg, 100%Cu	12.7 Hours	Thermal & 1 keV Resonance	511 (Positron)
^{115}In (n,n')^{115m}In	25 mg, 100% In	4.486 Hours	0.5 MeV Threshold	336.3
^{47}Ti (n,p)^{47}Sc ^{46}Ti (n,p)^{46}Sc ^{48}Ti (n,p)^{48}Sc	157 mg, 100% Ti	3.349 Days 83.81 Days 43.7 Hours	1.0 MeV Threshold 3.5 MeV Threshold 5.5 MeV Threshold	159.4 1121,889 984,1312,1038
^{58}Ni (n,p)^{58}Co	286 mg, 100% Ni	70.88 Days	1.2 MeV Threshold	811
^{64}Zn (n,p)^{64}Cu	117 mg, 100% Zn	12.7 Hours	1.5 MeV Threshold	511 (Positron)
^{54}Fe (n,p) ^{54}Mn ^{56}Fe (n,p) ^{56}Mn	132 mg, 100% Fe	312.2 Days 2.578 Hours	1.5 MeV Threshold 5.0 MeV Threshold	834.8 847
^{93}Nb (n, 2n)^{92m}Nb	270 mg, 100%Nb	10.13 Days	6.0 MeV Threshold	935

Co-normalization of the NW lobe power for the three separate reactor runs was accomplished using the measured activation of the same type of copper/gold flux wires in each of the four even-numbered core fuel elements surrounding the NW flux trap (Elements 32, 34, 36, 38). Each wire was placed in the circled position the middle of each element as shown in Figure 6, at the axial core midplane. Finally, a second set of foil positioning strips was prepared for Irradiation 2, with flux wires in the various positions as before, but without foil packages. This arrangement represents the assumed "unperturbed" LIPT configuration that is associated with the spectral unfolding and adjustment process.

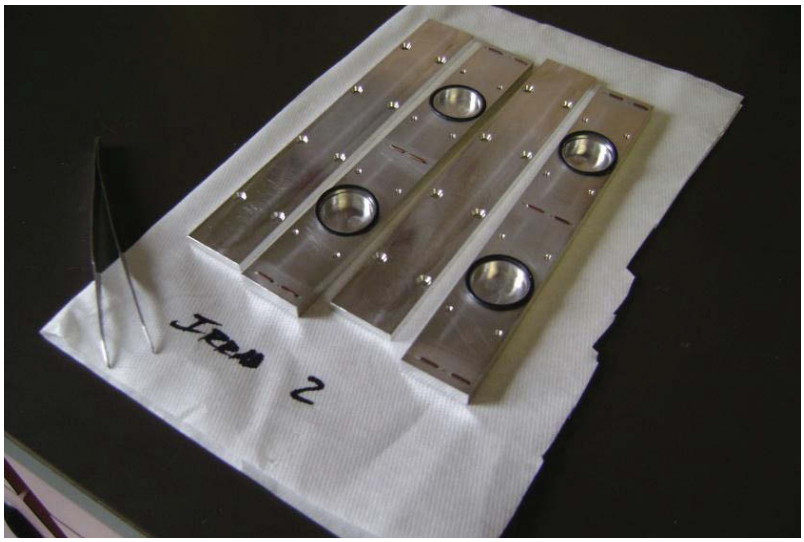

Figure 4. Foil positioning strips and covers for the bare and cadmium-covered foil packages. Foils are placed in the circular indentations and duplicate flux wires are placed in the indented slots at each end and in the middle of each strip.

Figure 5. Foil positioning strips and dummy strips mounted in their insert fitting on the right, which is then positioned in the NW LIPT test train insert on the left.

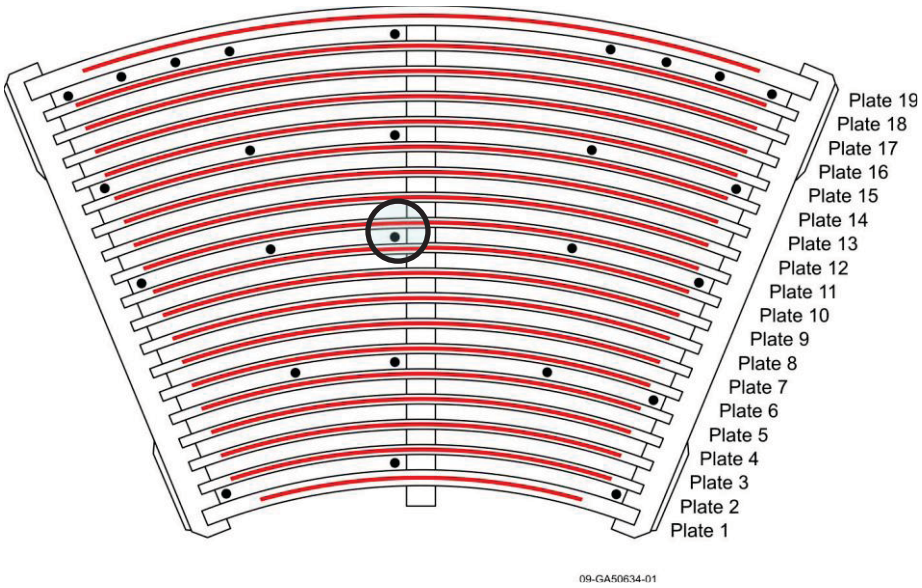

Figure 6. Transverse section of an ATRC fuel element showing available flux wire positions. The circled position in the center was used for power normalization in Irradiations 1-3 as discussed in the text.

For the third irradiation, the package of threshold interaction foils was suspended at the center of the boron spectral shifting shield, which was then placed in a second insert fitting as shown in Figure 7. The spectral shifter was a hollow sphere of sintered boron, enriched to approximately 90% in ^{10}B, with an inside diameter of approximately 2.5 cm (1”), an outside diameter of 5 cm (2”), and a nominal mass of 115 grams. This device prevents essentially all neutrons having energies of less than about 10 keV from reaching the foil package inside, effectively eliminating interfering interactions from thermal and resonance neutron interactions in the enclosed foils. The insert fitting for Irradiation 3 has 8 positions for flux wires as shown in Figure 7.

The cylindrical NW LIPT insert was positioned in a “Test Train”, which consists of the insert with one or the other of its two fittings described previously plus several hollow aluminum spacer sections that are assembled together axially and then put inside of an aluminum shroud that fits inside of the NW LIPT. Figure 8 illustrates how each test train is assembled for positioning in the NW LIPT with the center section aligned with the axial active core midplane.

Figure 7. Fitting for positioning of boron sphere. Duplicate flux wires are placed in the indented slots at each end, and just above and below the boron sphere. The two halves are then bolted together.

2.2 *A-Priori* Computational Model

An MCNP5 full-core model of the ATRC was developed for primary support of the validation protocol during the initial stage of development. This model is similar to the published full core ATR1994 Core Internals Changeout (CIC) Benchmark model [10], but modified to match the current configuration of the ATRC, which is somewhat different from the ATR configuration as a result of evolutionary changes in the ATR over the course of several core internal change-outs (CICs) and fuel design changes. Neutronically, the most significant differences between the cores are the fuel design, operating conditions and the flux trap loadings. ATRC fuel element plates are uniformly loaded with boron, whereas the ATR uses boron for power peaking control only in the four innermost and four outermost plates of the fuel elements. Furthermore, the ATR operates at a high power density with forced cooling under pressurized conditions, while the ATRC is an unpressurized pool type reactor that operates at a power generally less than 1 kW with cooling by natural convection. Hence, ATRC coolant is full density water, and the coolant, moderator (water and beryllium) and fuel can be assumed to remain at room temperature [13]. The other significant differences between the ATR and ATRC are related to the contents of the irradiation positions. Flux trap contents can not only influence core reactivity but also the relative power partitioning among the five core lobes. For the experiments discussed here the contents of the NW LIPT were as shown in Figure 8. For the remaining flux traps, various INL Test Plan documents and other resources were used to identify the current contents.

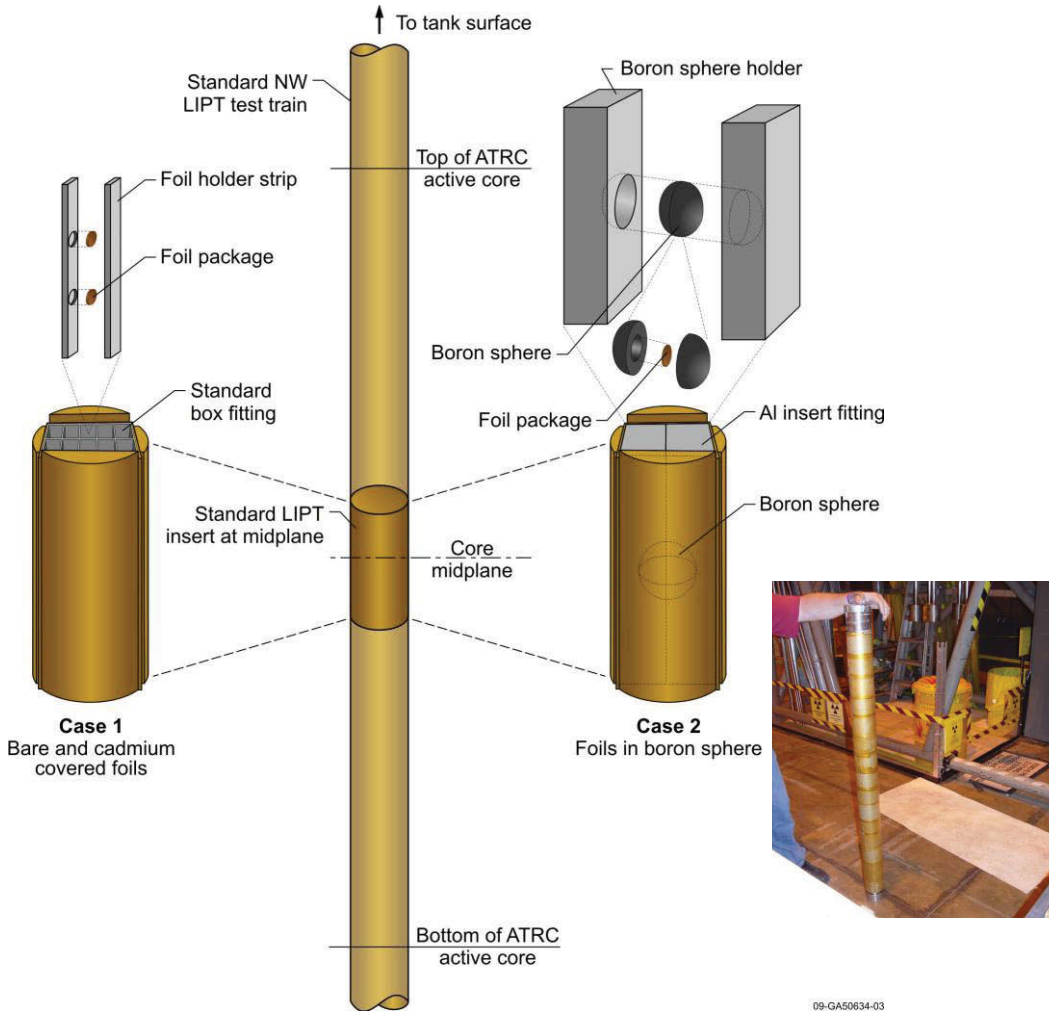

Figure 8. Positioning of test train components in the ATRC Northwest Large In-Pile Tube insert. The inset photo shows the entire assembled test train. Case 1 was the configuration for Irradiations 1 and 2. Case 2 was the configuration for Irradiation 3.

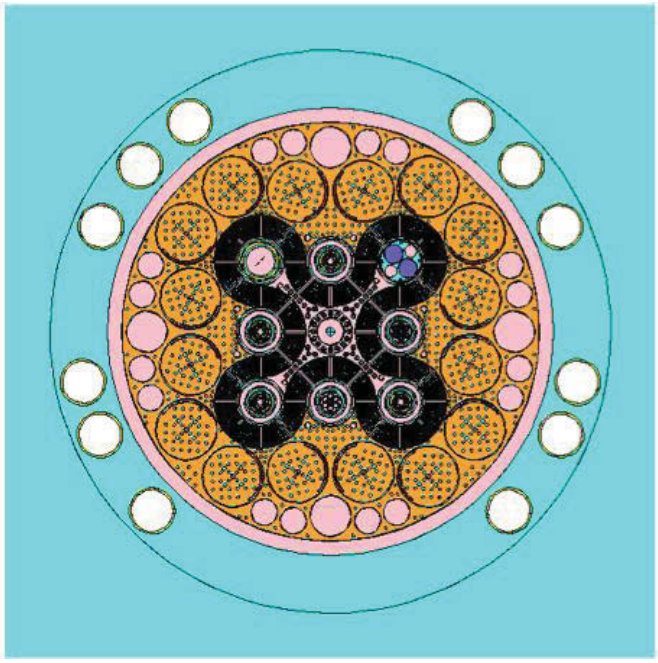

Figure 9. MCNP5 ATRC model geometry at the axial core mideplane.

A diagram of the MCNP5 model for Irradiation 1 is shown in Figure 9, above. The calculated K_{eff} for this critical configuration was 0.98928 ± 0.00002, where the quoted uncertainty is for the Monte Carlo convergence statistics alone. Separate TSUNAMI analyses indicate that the ATR model is also subject to approximately 0.5% additional uncertainty on the computed eigenvalue due to nuclear data uncertainty propagation. The individual Cu/Au wires and foils were explicitly modeled in their various locations to calculate fluxes and reaction rates at those positions. The reaction rates were tallied using the recent International Reactor Dosimetry File (IRDF) cross-section libraries [14]. The effective microscopic self-shielded and mutually-shielded cross-sections for the foils and wires were then determined by dividing the MCNP5 calculated reaction rate tally by the flux tally. Each tally was partitioned into the 47 energy groups corresponding to the BUGLE series of standard cross section libraries [15] plus one extra group to cover the highest energy range between 17.3 MeV and 20 MeV. The resulting dosimeter cross-sections were then used for various spectral adjustment analyses described in the following section.

3.0 MEASURED ACTIVATION AND SPECTRAL ADJUSTMENT RESULTS

The first two irradiations were successfully conducted in late September 2010 at the ATRC. Irradiation 3 was conducted in late April 2011. The absolute activities of the foils and wires were measured at the INL Radiation Measurements Laboratory (RML) according to standard RML procedures using HPGe gamma spectrometers. Some detailed results for the first three irradiations combined are summarized here.

3.1 Measured Foil and Wire Responses

Table 2 shows the measured saturation activities per atom for all foils whose responses were used in the spectral adjustment procedures reported here. Some of the responses of interest listed in Table 1 were too weak to measure accurately, so they were not used since they would effectively be weighted out of the least-squares adjustment algorithm anyway. The measured results are arranged in descending order of their primary energy range of neutron sensitivity. Total activity measurement uncertainties (counting statistics plus detector calibration) are in the range of 4-6% (1σ) for the foils used in Irradiation 1 and 6-10% for those used in Irradiation 3.

Table 3 shows the saturation activities for the Au/Cu flux wires in the NW LIPT hardware as well as in the four surrounding fuel elements in the case of Irradiation 1. The ratio of the gold activity relative to the copper activity for each wire is shown in the last column. This activity ratio, also referred to as a "spectral index" provides a simple indication of the relative "hardness" of the neutron spectrum to which the wire has been exposed. This is based on the fact that copper is relatively more sensitive to thermal neutrons compared to gold, which is roughly equally-sensitive to thermal and above-thermal neutrons.

In the case of a fully-thermalized neutron field this ratio will asymptotically approach the ratio of the Au and Cu cross sections at 2200 m/s, assuming no spatial self-shielding. This asymptotic ratio is approximately 22.1 (i.e. 98.74 barns divided by 4.47 barns). Any physically-realistic departure from the described asymptotic spectral conditions will cause the ratio to increase, primarily due to increased resonance capture in gold. For example it can be seen from Table 3 that the Au/Cu ratio is in the range of 51±3 in the upper and lower wire locations within the NW LIPT hardware since the spectrum is not fully thermalized. In the middle locations of the insert this ratio increases to approximately 60. This is an indication of the axial attenuation by aluminum of thermal neutrons streaming vertically into the NW LIPT insert from the water-filled regions above and below.

Irradiation 2 used the same configuration as Irradiation 1 except that the foil positions were empty - only the Cu/Au wires were installed in the NW LIPT hardware. The resulting wire activities were statistically identical to the corresponding Irradiation 1 activities at all locations in the NW LIPT hardware. This indicates that the presence of the foils and their cadmium covers has only a very small (if any) effect on the absolute flux and spectrum within the NW LIPT hardware.

The activities of the wires in the core fuel elements surrounding the NW LIPT were also essentially identical for the first two irradiations. This confirms that the NW lobe was operating at the same total power for both irradiations, as desired. Finally it is interesting to note from the spectral index data in Table 3 that the neutron spectrum in the core fuel elements is significantly harder than is the case within the NW LIPT. This is as expected, since the contents and surroundings of the NW LIPT provide some moderation of neutrons entering the LIPT region from the fuel.

Table 2. Measured foil saturation activities – ATRC Irradiations 1 and 3. Measurement uncertainties are as described in the text.

Response	Irradiation	Spectral Modifier	Measured σΦ
Nb(n,2n)	3	Boron Sphere	2.64E-19
Ti-48 (n,p)	3	Boron Sphere	1.35E-19
Fe-56 (n,p)	3	Boron Sphere	5.12E-19
Ti-46 (n,p)	3	Boron Sphere	5.00E-18
Ti-47 (n,p)	3	Boron Sphere	1.17E-17
Fe-54 (n,p)	3	Boron Sphere	4.10E-17
Zn-502 (n,p)	3	Boron Sphere	2.05E-17
Ni-1004 (n,p)	3	Boron Sphere	5.72E-17
In-(n,n')	3	Boron Sphere	1.30E-16
In(n,n')	1	Cadmium	1.24E-16
In(n,n')	1	Cadmium	1.23E-16
Cu(Res)	1	Cadmium	3.44E-16
Cu(Res)	1	Cadmium	3.54E-16
Mn(Res)	1	Cadmium	9.52E-16
Mn(Res)	1	Cadmium	1.01E-15
W(Res)	1	Cadmium	2.79E-14
W(Res)	1	Cadmium	2.86E-14
Au(Res)	1	Cadmium	4.90E-14
Au(Res)	1	Cadmium	5.09E-14
In(Res)	1	Cadmium	8.03E-14
In(Res)	1	Cadmium	8.57E-14
Au(Th)	1	None	1.07E-13
Au(Th)	1	None	1.09E-13
Mn(Th)	1	None	8.74E-15
Mn(Th)	1	None	8.26E-15

Table 4 shows the wire activities and spectral indices for Irradiation 3. The additional spectral hardening caused by the boron sphere is apparent from the spectral index data in the last column. In addition, it appears from the data for the core flux wires that the NW lobe was operating at a slightly higher power during Irradiation 3 compared to Irradiations 1 and 2, possibly due a slightly higher total reactor power, a slightly greater tilt of the power distribution toward the NW LIPT, or some combination of both. This information was used to renormalize the foil data from Irradiation 3 slightly downward when combining the Irradiation 3 foil activities with the corresponding foil data from Irradiation 1 to obtain a full range adjusted neutron spectrum (the foil activities shown in Table 2 reflect this renormalization).

Table 3. Measured flux wire saturation activities – ATRC Irradiation 1.

Wire Location[1]	^{197}Au(n,γ) σΦ (±3%)	^{63}Cu(n,γ) σΦ (±3%)	Spectral Ratio Au/Cu (±5%)
NW LIPT Upper 1L	1.70E-13	3.36E-15	50.41
NW LIPT Upper 1R	1.76E-13	3.29E-15	53.47
NW LIPT Upper 2L	1.74E-13	3.33E-15	52.32
NW LIPT Upper 2R	1.60E-13	3.11E-15	51.53
NW LIPT Middle 1L	1.61E-13	2.62E-15	61.25
NW LIPT Middle 1R	1.58E-13	2.73E-15	57.87
NW LIPT Middle 2L	1.63E-13	2.68E-15	60.60
NW LIPT Middle 2R	1.51E-13	2.65E-15	57.08
NW LIPT Lower 1L	1.75E-13	3.71E-15	47.21
NW LIPT Lower 1R	1.73E-13	3.42E-15	50.63
NW LIPT Lower 2L	1.71E-13	3.56E-15	47.89
NW LIPT Lower 2R	1.83E-13	3.64E-15	50.36
LIPT Average	**1.68E-13**	**3.18E-15**	**52.86**
Fuel Element 32	1.58E-13	1.64E-15	96.23
Fuel Element 34	1.13E-13	1.14E-15	99.06
Fuel Element 36	9.07E-14	8.73E-16	103.84
Fuel Element 38	1.36E-13	1.30E-15	104.40
Core Average	**1.24E-13**	**1.24E-15**	**100.37**

[1] Location "Upper 1L" denotes the wire position at the upper end of Foil Strip 1, Left Side, etc.

3.2 Spectral Adjustment and Code Validation Analysis

Table 5 shows an 8-group adjusted neutron spectrum for the NW LIPT corresponding to the foil measurement results of Irradiation 1 combined with those of Irradiation 3. The adjusted spectrum was determined using a variance-weighted overdetermined least-square procedure specifically adapted by the INL for this type of application [12]. All 25 measured responses listed in Table 2 were used for the adjustment. There were 7 duplicate responses and 1 triplicate response (^{115}In(n,n')), for a net total of 16 responses with sufficient linear independence on the specified 8-group energy structure. The elements of the 25 x 8 coefficient matrix and the *a-priori* flux vector for the adjustment procedure were computed using the MCNP5 model of the experimental apparatus described earlier The nature of the adjustment algorithm is such that the fluxes shown in Table 6 represent a variance-weighted least-squares best estimate spatial average flux over the four foil positions in the NW LIPT apparatus, corrected for the perturbing effect of the cadmium covers, the boron sphere, and the foils themselves.

Table 4. Measured flux wire saturation activities – ATRC Irradiation 3.

Wire Location[1]	^{197}Au(n,γ) σΦ (±3%)	^{63}Cu(n,γ) σΦ (±3%)	Spectral Ratio Au/Cu (±5%)
NW LIPT Upper L	1.69E-13	3.14E-15	53.96
NW LIPT Upper R	1.69E-13	3.12E-15	54.25
NW LIPT Upper Middle L	1.35E-13	1.99E-15	67.73
NW LIPT Upper Middle R	1.26E-13	1.98E-15	63.57
NW LIPT Lower Middle L	1.32E-13	2.00E-15	66.12
NW LIPT Lower Middle R	1.30E-13	2.02E-15	64.49
NW LIPT Lower L	1.70E-13	3.12E-15	54.59
NW LIPT Lower R	1.73E-13	3.20E-15	53.97
LIPT Average	**1.51E-13**	**2.57E-15**	**58.58**
Fuel Element 32	1.88E-13	1.84E-15	102.06
Fuel Element 34	1.29E-13	1.28E-15	100.52
Fuel Element 36	9.88E-14	1.01E-15	97.96
Fuel Element 38	1.47E-13	1.44E-15	102.37
Core Average	**1.41E-13**	**1.39E-15**	**101.04**
Core Average Irr 3/Irr 1	**1.13 (±5%)**	**1.12 (±5%)**	**-**

[1] Location "Upper L" denotes the upper left-hand flux wire position, etc.

The bias of the *a-priori* model for the conditions being calculated is the difference between the *a-priori* flux and the adjusted flux, with its corresponding uncertainty. It can be seen that in this case the adjustment tended to reduce the total flux by about 18% with a concurrent small degree of softening (shift toward the lower-energy groups) that appears to be of limited statistical significance. The chi-squared parameter for the adjustment shows an excellent fit, with a possible indication of over-conservatism in the quantification of uncertainty in the underlying foil reaction rate measurements. Table 6 shows the measured, *a-priori*, and adjusted foil saturation activities for this case. It can be seen that the adjusted activities are very consistent with the corresponding measurements.

4.0 FUTURE WORK

A fourth irradiation was also completed during 2011, with a focus on more detailed flux spectrum measurements and power distribution measurements in the core fuel elements using Au/Cu and ^{235}U/Al flux wires, respectively. A summary of key results for these measurements is available in [16].

Table 5. Eight-group neutron flux spectrum from foils – Northwest Large In-Pile Tube, Irradiations 1 and 3 combined, 600W. MCNP5 *a-priori.*

Energy Group	Upper E (eV)	Lower E (eV)	*A-Priori* Flux (n/cm**2-s)	Adjusted Flux (n/cm**2-s)	Propagated Uncertainty (1σ)
1	2.00E+07	1.92E+05	2.95E+08	2.70E+08	4.53%
2	1.92E+05	2.97E+05	8.13E+08	5.95E+08	13.5%
3	2.97E+05	4.54E+02	9.59E+08	7.54E+08	6.20%
4	4.54E+02	3.73E+01	2.95E+08	3.23E+08	8.05%
5	3.73E+01	1.07E+01	1.45E+08	1.35E+08	3.32%
6	1.07E+01	1.86E+00	1.98E+08	1.51E+08	4.51%
7	1.86E+00	4.14E-01	1.81E+08	1.37E+08	4.77%
8	4.14E-01	1.0000E-05	9.64E+08	8.11E+08	3.49%
Total Fast Flux (Groups 1-7)	2.0000E+07	4.1399E-01	2.89E+09	2.36E+09	4.14%
Fast/Thermal Ratio			3.00	2.91	5.41%

Note: X^2 per degree of freedom = 0.86

For the longer term, fabrication of an additional set of foil and wire positioning devices was also recently completed for use in the Southeast In-Pile Tube (SE IPT), diametrically across the reactor core from the NW LIPT. The new SE IPT hardware contains one foil positioning strip, identical to the ones used in the NW LIPT hardware and is designed to contain the same foil sets. Two additional spectral measurements will be conducted with this new apparatus, along with the NW LIPT apparatus, in place.

In both of the additional irradiations still to be conducted, the experiment hardware and the core fuel elements will also be heavily instrumented with Au/Cu and U/Al wires. Various least-squares techniques for statistically combining the ^{235}U fission rate with the Au and Cu capture rates at each instrumented flux trap and core fuel location to produce an improved estimate for the adjusted neutron flux spectrum at these positions that is statistically tied to the local fission rate will be explored. Taken together, the six irradiations will serve as the basis for flexible and repeatable validation experiment protocols applicable to all of the computational neutron transport tools included in the new suite

Table 6. Measured, *a-priori*, and adjusted foil interaction rates for Irradiations 1 and 3 combined.

Response	Spectral Mod.	Measured σΦ	*A-Priori* σΦ	Adjusted σΦ
Nb(n,2n)	Boron Sphere	2.64E-19	2.50E-19	2.29E-19
Ti-48 (n,p)	Boron Sphere	1.35E-19	1.62E-19	1.48E-19
Fe-56 (n,p)	Boron Sphere	5.12E-19	6.03E-19	5.51E-19
Ti-46 (n,p)	Boron Sphere	5.00E-18	6.08E-18	5.56E-18
Ti-47 (n,p)	Boron Sphere	1.17E-17	1.14E-17	1.02E-17
Fe-54 (n,p)	Boron Sphere	4.10E-17	4.71E-17	4.30E-17
Zn-502 (n,p)	Boron Sphere	2.05E-17	2.25E-17	2.06E-17
Ni-1004 (n,p)	Boron Sphere	5.72E-17	6.37E-17	5.77E-17
In-(n,n')	Boron Sphere	1.30E-16	1.46E-16	1.24E-16
In(n,n')	Cadmium	1.24E-16	1.48E-16	1.26E-16
In(n,n')	Cadmium	1.23E-16	1.48E-16	1.25E-16
Cu(Res)	Cadmium	3.44E-16	4.37E-16	3.47E-16
Cu(Res)	Cadmium	3.54E-16	4.42E-16	3.50E-16
Mn(Res)	Cadmium	9.52E-16	1.07E-15	9.83E-16
Mn(Res)	Cadmium	1.01E-15	1.07E-16	9.79E-16
W(Res)	Cadmium	2.79E-14	3.02E-14	2.78E-14
W(Res)	Cadmium	2.86E-14	3.11E-14	2.87E-14
Au(Res)	Cadmium	4.90E-14	6.42E-14	5.08E-14
Au(Res)	Cadmium	5.09E-14	6.24E-14	4.94E-14
In(Res)	Cadmium	8.03E-14	1.09E-13	8.31E-14
In(Res)	Cadmium	8.57E-14	1.09E-13	8.29E-14
Au(Th)	None	1.07E-13	1.31E-13	1.07E-13
Au(Th)	None	1.09E-13	1.32E-13	1.07E-13
Mn(Th)	None	8.74E-15	1.01E-14	8.55E-15
Mn(Th)	None	8.26E-15	1.01E-14	8.52E-15

ACKNOWLEDGMENTS

This work was sponsored by the United States Department of Energy through the Idaho National Laboratory Advanced Test Reactor Life Extension Program under DOE Idaho Operations Office Contract DE-AC07-05ID14517

REFERENCES

1. T. Goorley, et. al., Release of MCNP5_RSICC_1.30, MCNP Monte Carlo Team X-5, LA-UR-04-4519, Los Alamos National Laboratory, November 2004 and, X-5 Monte Carlo Team, MCNP—A General Monte Carlo N-Particle Transport Code, Version 5, Volume I, LA-UR-03-1987, Los Alamos National Laboratory, USA (2003).

2. C.J. Pfeifer, "PDQ Reference Manual II", WAPD-TM-947(L) (1971).

3. "NJOY99- Code System for Producing Pointwise and Multigroup Neutron and Photon Cross Sections from ENDF/B Data" and "AMPX77- Modular Code System for Generating Coupled Multigroup Neutron-Gamma Libraries from ENDF/B", Radiation Safety Information Computational Center, Oak Ridge National Laboratory, USA, http://www-rsicc.ornl.gov (2010).

4. D.F. Hollenbach, L.M. Petrie, N.F. Landers, "KENO-VI: A General Quadratic Version of the KENO Program", ORNL/TM-13011, Oak Ridge National Laboratory, USA (1996).

5. B.L. Broadhead, B.T. Rearden, C.M. Hopper, J.J. Wagschal, C.V. Parks, "Sensitivity- and Uncertainty-Based Criticality Safety Validation Techniques," *Nucl. Sci. Eng.* **146**, 340–366 (2004).

6. S.M. Bowman (Ed.), "SCALE: A Modular Code System for Performing Standardized Computer Analyses for Licensing Evaluation, ORNL/TM-2005/39, Oak Ridge National Laboratory, USA (2009).

7. Studsvik Scandpower, "HELIOS Methods (Version 1.10)" (2008).

8. J.M. McGhee, T.A. Wareing, D.J. Barnett, "ATTILA Version 5: User Manual", Transpire Inc., Gig Harbour WA, USA (2006).

9. M.D. DeHart, "Advancements in Generalized-Geometry Discrete Ordinates Transport for Lattice Physics Calculations", *Proc. of PHYSOR–2006, American Nuclear Society Topical Meeting on Reactor Physics: Advances in Nuclear Analysis and Simulation*, Vancouver B.C., Canada, September 10–14, 2006, Paper A154, (2006).

10. S.S. Kim, B.G. Schnitzler, "Advanced Test Reactor: Serpentine Arrangement of Highly Enriched Water-Moderated Uranium-Aluminide Fuel Plates Reflected by Beryllium" HEU-SOLTHERM-022, *International Handbook of Evaluated Criticality Safety Benchmark Experiments*, NEA/NSC/DOC(95)03, OECD-NEA (2008).

11. JW Rogers, R.A. Anderl, "ATR Neutron Spectral Characterization", INEL-95/0494, Idaho National Laboratory, USA (1995).

12. D.W. Nigg, C.A. Wemple, R. Risler, J.K. Hartwell, Y.D. Harker, G.E. Laramore, "Modification of the University of Washington Neutron Radiography Facility for Optimization of Neutron Capture Enhanced Fast-Neutron Therapy, *Medical Physics* **27:**359-367 (2000).

13. J.D. Bess, "Preliminary Assessment of ATR-C Capabilities to Provide Integral Benchmark Data for Key Structural/Matrix Materials that May be Used for Nuclear Data Testing and Analytical Methods Validation", INL/EXT-09-15591, Idaho National Laboratory, USA (2009).

14. P.J. Griffin and R. Paviotti-Corcuera, "Summary Report of the Final Technical Meeting on "International Reactor Dosimetry File: IRDF-2002", International Atomic Energy Agency, INDC(NDS)-448 (2003)

15. R.W. Roussin, "BUGLE-80 Coupled 47-Neutron, 20 Gamma-Ray P3 Cross Section Library", DLC-75, Radiation Shielding Information Center, Oak Ridge National Laboratory, USA (1980).

16. D.W. Nigg, J.W. Nielsen, G.K. Taylor, "Validation Protocols to Support the Neutronics Modeling, Simulation, and V&V Upgrade for the Advanced Test Reactor", In Publication, Transactions of the ANS 2102 Annual Meeting, Chicago, Illinois (2012).